Electronic band structures and magnetism of intermetallic manganese compounds Mn_4X (X identical to N, C)

1991 J. Phys.: Condens. Matter 3 1753

(http://iopscience.iop.org/0953-8984/3/12/006)

J. Phys.: Condens. Matter 3 (1991) 1753–1761. Printed in the UK

Electronic band structures and magnetism of intermetallic manganese compounds Mn_4X (X ≡ N, C)

Yukio Tagawa and Kazuko Motizuki
Department of Material Physics, Faculty of Engineering Science, Osaka University, Toyonaka 560, Japan

Received 16 July 1990

Abstract. Electronic band structures of intermetallic manganese compounds, Mn_4N and Mn_4C, having the cubic perovskite-type crystal structure are calculated for the non-magnetic state by a self-consistent augmented-plane-wave (APW) method. The energy dispersion, the density of states and the Fermi surface are shown. The bonding nature between Mn atoms and N or C atoms is discussed by calculating bond orders. The band structure for the ferrimagnetic state of Mn_4N is also calculated by the APW method. The calculated magnetic moments and the electronic specific heat coefficient in the ferrimagnetic state are compared with the observed results.

1. Introduction

Intermetallic manganese compounds, Mn_4N and Mn_4C, have cubic perovskite-type crystal structure, Mn atoms being at the corners and the face centres (these are labelled as Mn(I) and Mn(II), respectively) and N and C atoms at the body centre. These compounds have attracted much interest because the different local environments of Mn(I) and Mn(II) atoms are reflected in various physical properties of these compounds as follows.

(i) Mn_4N becomes a ferrimagnet below $T_N = 756$ K (Takei *et al* 1962, Mekata 1962, Fruchart *et al* 1979) and the magnetic moments of Mn(I) and Mn(II) are observed to be different and antiparallel. The magnitude of the moments of the Mn(I) atoms is four times that of Mn(II) atoms. The non-collinear component in the magnetic structure of Mn_4N has also been reported (Fruchart *et al* 1979).

(ii) In a mixed compound $Mn_4N_{0.75}C_{0.25}$ which becomes a ferrimagnet below $T_N = 850$ K, it has been observed that the total moment and the moment of Mn(II) decrease and increase, respectively, by a replacement of N atoms by C atoms, while the moment of Mn(I) changes little (Takei *et al* 1962).

(iii) The Mn(II) atoms which surround the N or C atoms octahedrally are strongly bonded to the N or C atoms. Therefore Mn(II) atoms are chemically stable. On the other hand, the Mn(I) atoms are easily substituted by Zn, Ga, Sn, etc, giving rise to the family of compounds, Mn_3MN or Mn_3MC (M ≡ Zn, Ga, Sn, etc).

(iv) Mn_4N is stable below 1150 K, while Mn_4C is unstable at room temperature (Morgan 1954).

0953-8984/91/121753 + 09 $03.50

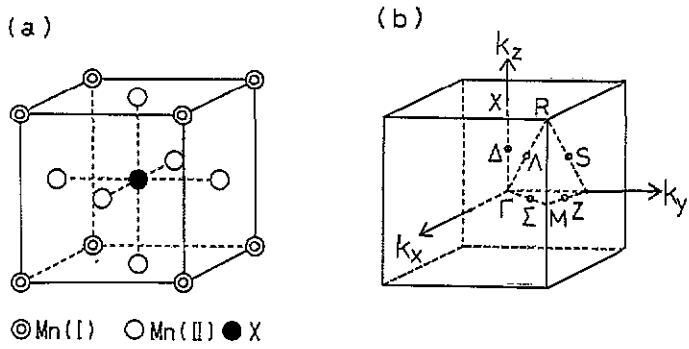

Figure 1. (*a*) Cubic perovskite-type crystal structure. (*b*) Brillouin zone for the cubic lattice with symmetry points.

To understand the physical properties of Mn_4N and Mn_4C the electronic band structure of these compounds holds the key. In the present stage, however, little is known about the electronic bands of Mn_4N and Mn_4C. Previously, we have made band calculations for non-magnetic Mn_3MC (M ≡ Zn, Ga, In, Sn) (Motizuki and Nagai 1988) and have found that the Mn d electrons in these compounds should be treated not as localized electrons but as itinerant electrons because the Mn d band is fairly wide.

In this paper we have calculated the electronic bands for the non-magnetic state of Mn_4N and Mn_4C and for the ferrimagnetic state of Mn_4N, by a self-consistent augmented plane-wave (APW) method. The computational details are described in section 2. In section 3 the dispersion curves, the densities of states and the Fermi surfaces are calculated for the non-magnetic state. Calculations of the bond orders are also carried out for the non-magnetic state of Mn_4N to elucidate the bonding nature of the Mn atoms and the N atoms. The results of the ferrimagnetic band calculation are given in section 4. The calculated magnetic moments are compared with the observed results. Furthermore we estimate the coefficient of the electronic specific heat from the density of states at the Fermi level. The results are discussed in connection with observations.

2. Electronic band calculation

The crystal structure and the Brillouin zone of Mn_4X (X ≡ N, C) are shown in figures 1(*a*) and 1(*b*), respectively. We adopt the muffin-tin approximation to the potential. The local-density approximation (Gunnarsson and Lundqvist 1976) is used to construct the exchange and correlation terms of the one-electron potential. We use the criterion that $l_{max} = 8$ and $|\boldsymbol{k} + \boldsymbol{G}|_{max} = (2\pi/a) \times 5$ ($\boldsymbol{k}$ being a vector in the Brillouin zone of figure 1(*b*) and $\boldsymbol{G}$ a reciprocal lattice vector). We have determined self-consistently the charge density of the crystal using a set of four special points $(\frac{1}{8}, \frac{1}{8}, \frac{1}{8})$, $(\frac{3}{8}, \frac{1}{8}, \frac{1}{8})$, $(\frac{3}{8}, \frac{3}{8}, \frac{1}{8})$, $(\frac{3}{8}, \frac{3}{8}, \frac{3}{8})$ in the iteration process (Chadi and Cohen 1973). The starting charge density has been constructed by superposing the self-consistent charge densities of the neutral atoms: Mn $3d^5 4s^2$, N $2s^2 2p^3$ and C $2s^2 2p^2$. The cores are considered to be frozen. We have calculated the energy bands of Mn_4N and Mn_4C within an accuracy

Table 1. Lattice parameters and muffin-tin radii used in the band calculations of Mn_4X ($X \equiv N, C$).

	Lattice parameter a (Å)	Muffin-tin radii (in units of a)		
		Mn(I)	Mn(II)	X
Mn_4N	3.865	0.250	0.245	0.249
Mn_4C	3.865	0.249	0.240	0.250

of 0.002 Ryd. In table 1 the lattice parameters and the muffin-tin radii of Mn, N and C spheres used in the present calculation are listed. The density of states has been calculated by the linear energy tetrahedron method (Jepsen and Andersen 1971, Lehmann and Taut 1972) using the energy eigenvalues at 35 points in the one-fortyeighth Brillouin zone.

3. Non-magnetic state

The dispersion curves of the non-magnetic energy bands of Mn_4X ($X \equiv N$, C) along the symmetry lines are shown in figure 2. The lowest band consists of the X 2s states. The bands above the gap are mixed bands of the X 2p and Mn 3d states.

The densities of states calculated for Mn_4X are shown in figure 3. Contributions arising from 3d orbitals of the Mn(I) and Mn(II) atoms and 2p orbitals of the X atoms, inside the muffin-tin spheres, are denoted separately. As seen in figure 3 the energy range of the p–d mixed bands of each compound can be divided into three parts:

(i) the low-energy part between 0.05 and 0.30 Ryd for Mn_4N and that between 0.15 and 0.45 Ryd for Mn_4C;

(ii) the intermediate-energy range between 0.30 and 0.70 Ryd for Mn_4N and that between 0.45 and 0.75 Ryd for Mn_4C;

(iii) the high-energy part above 0.70 Ryd for Mn_4N and that above 0.75 Ryd for Mn_4C.

We have found that the X 2p orbitals are mixed significantly with the Mn 3d orbitals in parts (i) and (iii), but not in part (ii). Therefore, part (i) and part (iii) may correspond to bonding and anti-bonding bands of the X 2p orbitals and the Mn 3d orbitals, respectively. The Mn 3d orbitals in these parts arise mainly from the Mn(II) atoms. In part (ii), the 3d orbitals of Mn(I) are mixed with those of Mn(II). The Fermi level is located in the part (ii). The width of the mixed band, part (ii), arising from the 3d orbitals of Mn(I) and Mn(II) atoms is about 0.4 Ryd for Mn_4N and 0.3 Ryd for Mn_4C, which are fairly wide. Therefore, we can conclude that the Mn 3d electrons in these compounds should be treated not as localized electrons but as itinerant electrons.

We have constructed the Fermi surface of each compound by the method of three-dimensional interpolation using a spline function. The results are shown in figure 4. The Fermi surface of Mn_4N or Mn_4C consists of three parts: the hole surface around the Γ point shown in figure 4(a), the hole surface around the R point shown in figure 4(b), and the electron surfaces shown in figure 4(c).

From the calculated results we have found that the gross features of the dispersion curves and the density of states for Mn_4N are similar to those for Mn_4C, except that

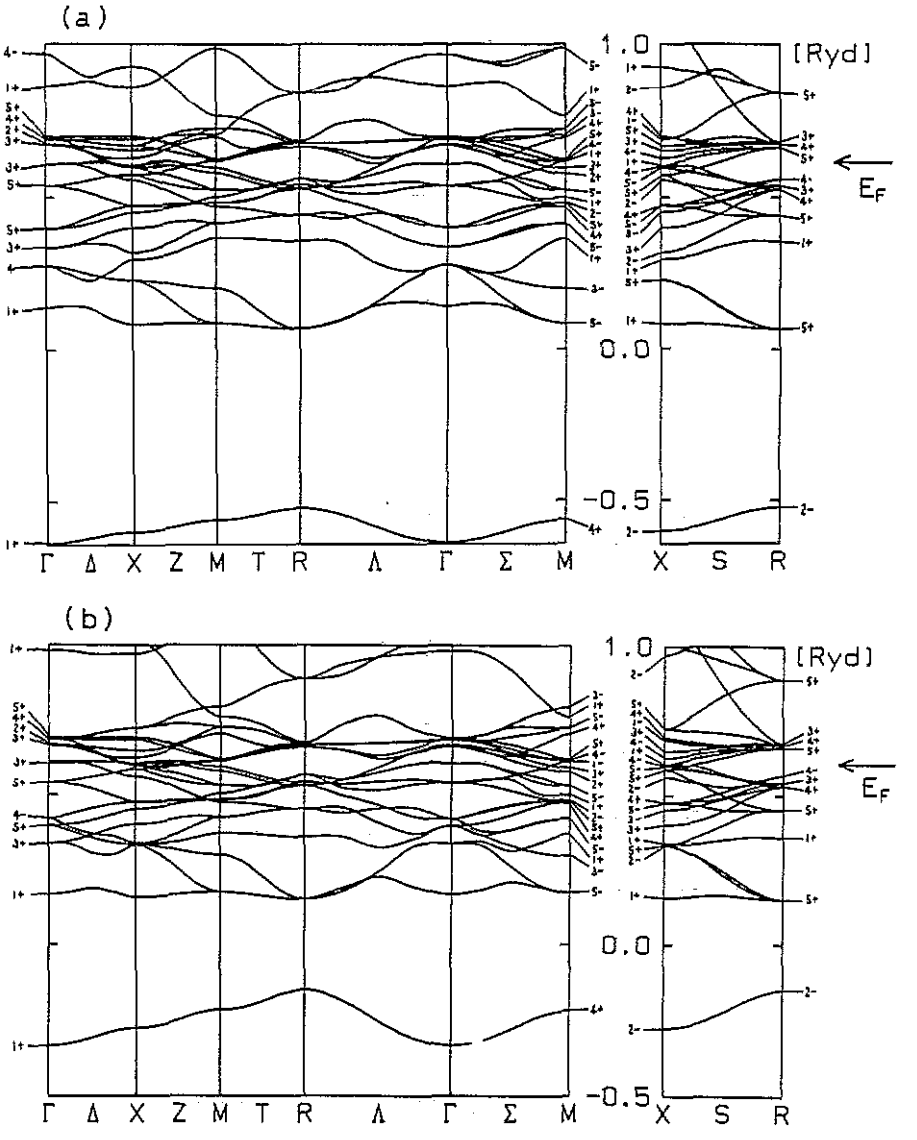

Figure 2. Dispersion curves of the non-magnetic bands of (*a*) Mn_4N and (*b*) Mn_4C.

the gap between the lowest band and the mixed bands of the N or C 2p and Mn 3d states and the overlap between the bonding and mixed bands are large for Mn_4N compared with those for Mn_4C. The difference between N and C atoms does not affect the overall shape of the density of states but leads to a shift of the Fermi level. The number of the valence electron of Mn_4N is larger by one than that of Mn_4C, and then the Fermi level of Mn_4N shifts to higher energies. Such a character is clearly reflected in the Fermi surfaces shown in figure 4, namely the electron and hole surfaces obtained for Mn_4N become small and large, respectively, for Mn_4C.

The bond order β for a wavefunction ψ between two atomic or atomic-like orbitals φ_i and φ_j centred on different nuclei is defined by (Suzuki *et al* 1988)

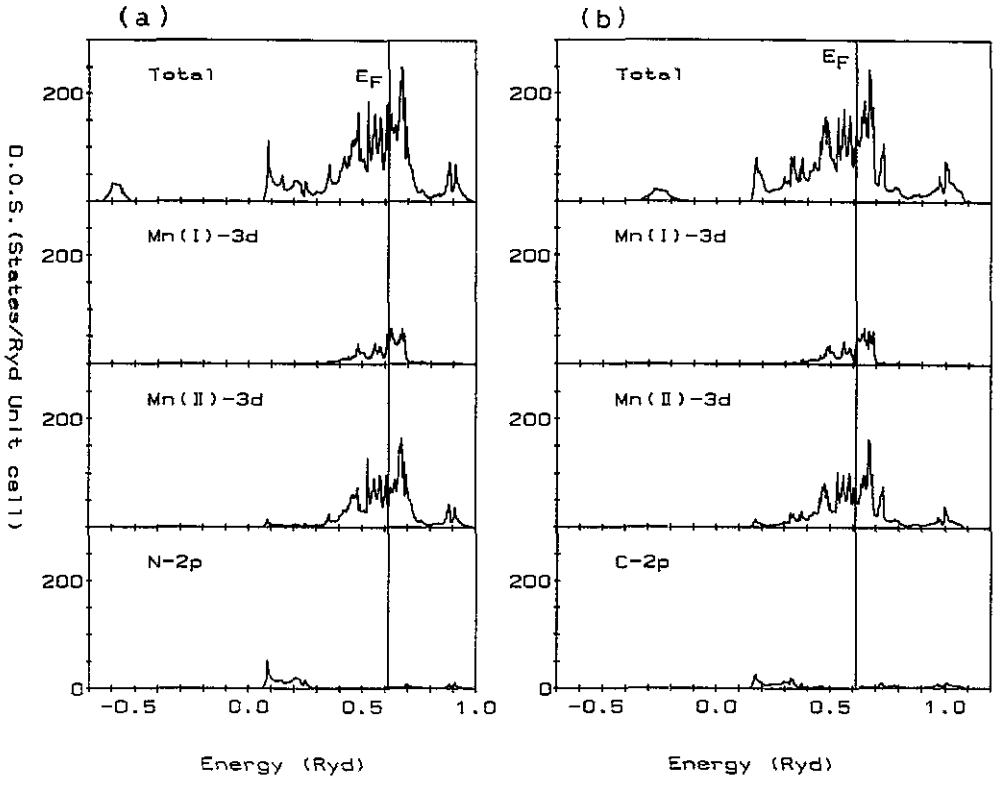

Figure 3. The densities of states of (*a*) Mn_4N and (*b*) Mn_4C for the non-magnetic state.

$$\beta_{ij}(n,k) = \tfrac{1}{2}[\langle\varphi_i|\psi_{n,k}\rangle\langle\psi_{n,k}|\varphi_j\rangle + \langle\varphi_j|\psi_{n,k}\rangle\langle\psi_{n,k}|\varphi_i\rangle]$$

where $\psi_{n,k}$ denotes the Bloch function obtained by the APW band calculation (n and k being the band suffix and wavevector, respectively). The bonding or anti-bonding nature is related to the sign of β_{ij}. We have calculated three types of bond order between the Mn(II) atom at $(0, \frac{1}{2}, \frac{1}{2})$ and the N atom at $(\frac{1}{2}, \frac{1}{2}, \frac{1}{2})$, as a function of k along the [1, 1, 0] line:

(1) $\beta_{\mathrm{Mn}d_{x^2},\mathrm{N}p_x}(n,k)$ between $\varphi^{d_{3x^2-r^2}}$ of Mn(II) and φ^{p_x} of N;
(2) $\beta_{\mathrm{Mn}d_{xy},\mathrm{N}p_y}(n,k)$ between $\varphi^{d_{xy}}$ of Mn(II) and φ^{p_y} of N;
(3) $\beta_{\mathrm{Mn}d_{zx},\mathrm{N}p_z}(n,k)$ between $\varphi^{d_{zx}}$ of Mn(II) and φ^{p_z} of N;

The results for $\beta_{\mathrm{Mn}d_{x^2},\mathrm{N}p_x}(n,k)$, $\beta_{\mathrm{Mn}d_{xy},\mathrm{N}p_y}(n,k)$ and $\beta_{\mathrm{Mn}d_{zx},\mathrm{N}p_z}(n,k)$ are shown in figures 5(*b*), 5(*c*) and 5(*d*), respectively. The values of β for the bands in the energy part (i) in figure 5(*a*) are positive, while those for the bands in the energy part (iii) are negative. The values of β for the bands in the energy part (ii) are almost zero and we omit β for these bands in figure 5. Therefore, the energy parts (i) and (iii) correspond to the bonding and anti-bonding bands between Mn(II) 3d and N 2p, respectively, and the energy part (ii) corresponds to the non-bonding bands. The absolute values of β decrease as the k-vector approaches the Γ point, since the mixing of the N 2p orbitals and the Mn(II) 3d orbitals vanishes completely at the Γ point.

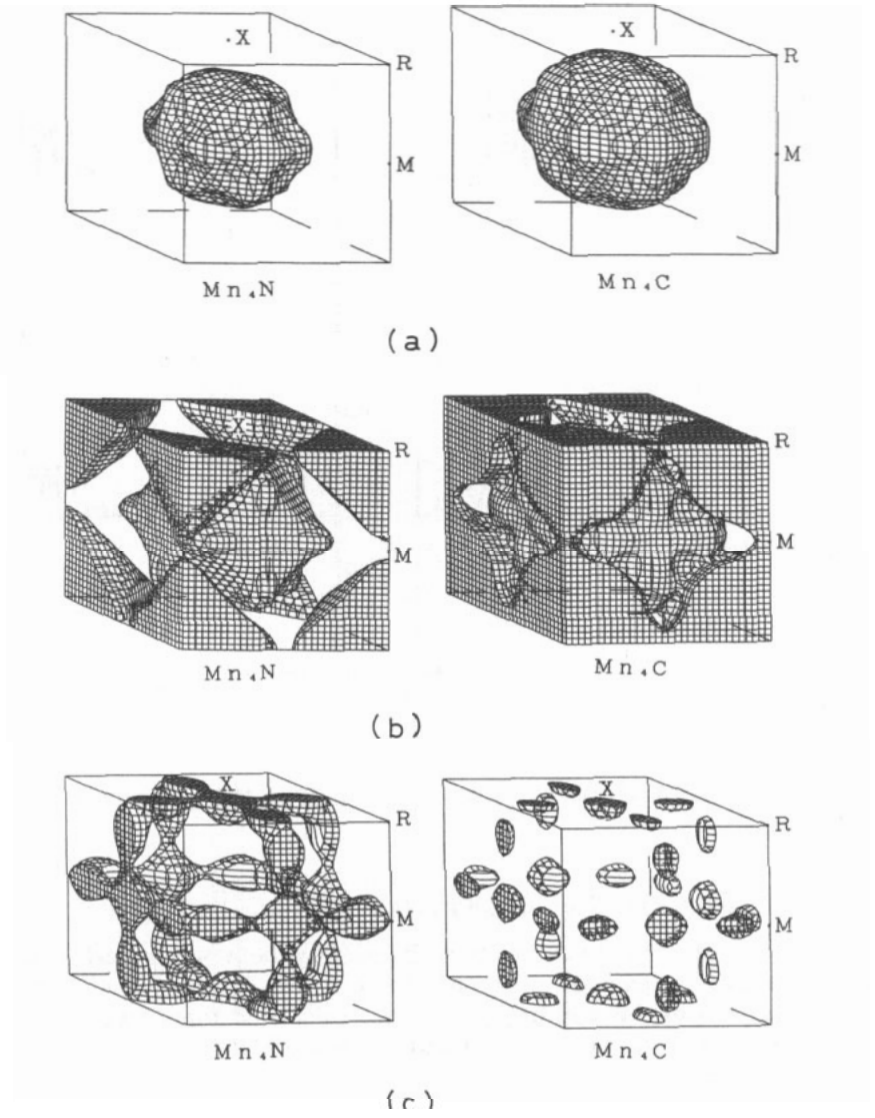

Figure 4. The Fermi surface of non-magnetic Mn_4X (X ≡ N, C): (*a*) hole surface; (*b*) hole surface; (*c*) electron surfaces.

The Mn(II) 3d states which are mixed with the N 2p states arise mainly from dγ orbitals for the bands denoted as 1, 2, 4, 6, 7, 8 and from dε orbitals for the bands denoted as 3, 5. The chemical bonding between the Mn(II) dγ and N 2p orbitals is as strong as that between Mn(II) dε and N 2p orbitals, but the energy splitting between the bonding and anti-bonding bands for Mn(II) dγ and N 2p is large compared with that for Mn(II) dε and N 2p. The bond orders between Mn(I) 3d and N 2p orbitals are small in each energy part and therefore the chemical bonding between Mn(I) and N is very weak.

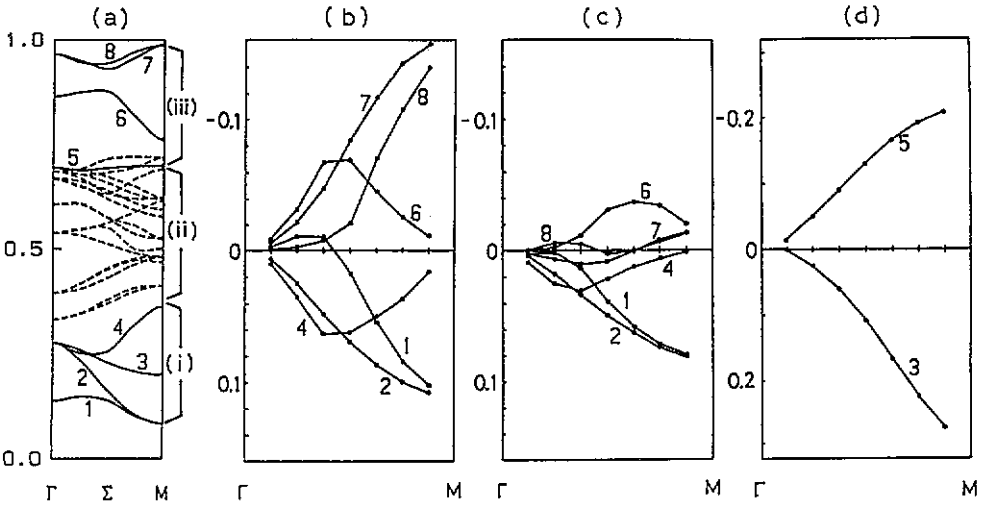

Figure 5. (*a*) The dispersion curves along the ΓM line, and (*b*)–(*d*) the bond orders (*b*) $\beta_{Mnd_{x^2},Np_x}(n,k)$, (*c*) $\beta_{Mnd_{xy},Np_y}(n,k)$ and (*d*) $\beta_{Mnd_{zx},Np_z}(n,k)$. The numbers attached to each line in (*b*), (*c*) and (*d*) denote the band suffices in (*a*).

4. Ferrimagnetic state

The ferrimagnetic energy bands of Mn_4N have been calculated by the self-consistent APW method. The starting electronic configurations of the Mn(I), Mn(II) and N atoms are taken to be different for spin-up and spin-down states as follows: $(3d)^4(4s)^1$ and $(3d)^1(4s)^1$ for up and down spins of Mn(I); $(3d)^2(4s)^1$ and $(3d)^3(4s)^1$ for up and down spins of Mn(II); $(2s)^1(2p)^{1.5}$ for both up and down spins of N. The densities of states for the spin-up and spin-down bands are shown in figure 6. Contributions arising from the Mn(I) 3d, Mn(II) 3d and N 2p states, inside each muffin-tin sphere, are shown separately in figure 6. Comparing the density of states for the ferrimagnetic state with that for the non-magnetic state shown in figure 3, we have found that the splitting between the spin-up and spin-down bands cannot be described by a rigid splitting of the non-magnetic band and the energy splitting of the spin-up and spin-down bands of Mn(I) is opposite to that of Mn(II). The total density of states at the Fermi level is obtained as 60.6 states Ryd^{-1}/unit cell and 22.3 states Ryd^{-1}/unit cell for the spin-up and spin-down bands, respectively. Contributions arising from the Mn(I) 3d and Mn(II) 3d and N 2p orbitals, inside each muffin-tin sphere, are 6.4 states Ryd^{-1}/atom, 14.4 states Ryd^{-1}/atom and 0.9 states Ryd^{-1}/atom for the spin-up band and 0.1 states Ryd^{-1}/atom, 6.6 states Ryd^{-1}/atom and 0.2 states Ryd^{-1}/atom for the spin-down band, respectively.

The magnetic moments inside the muffin-tin spheres at the Mn(I), Mn(II) and N sites are obtained as $3.02\mu_B$/atom, $-0.96\mu_B$/atom, $0.09\mu_B$/atom, respectively. The total magnetic moment is calculated to be $0.46\mu_B$/unit cell. The magnetic moment of Mn(I) is about three times that of Mn(II). As shown in figure 6, the densities of states of the spin-up and spin-down bands arising from Mn(I) 3d have peaks on the lower- and higher-energy sides of the Fermi level, respectively. The magnetic moment induced at N site originates from the difference between the degrees of p–d mixing for the

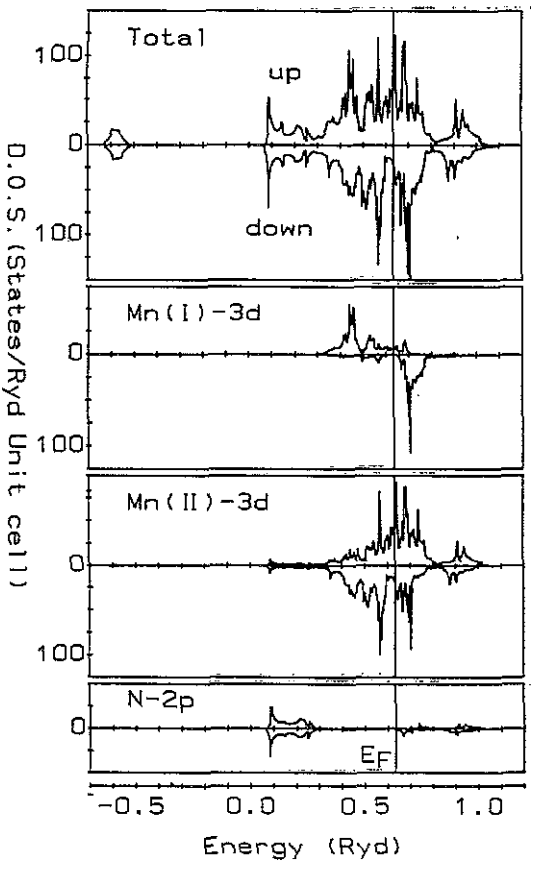

Figure 6. The density of states of Mn_4N for the ferrimagnetic state.

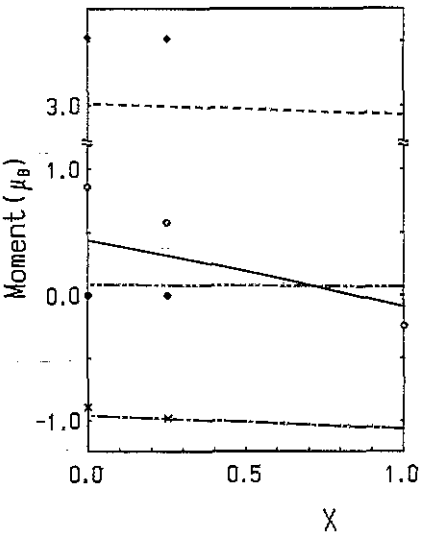

Figure 7. The magnetic moments calculated for the mixed compounds $Mn_4N_{1-x}C_x$ (——, total; – – –, Mn(I); — — —, Mn(II); — · — · —, N) and the observed magnetic moments at 300 K (○, total; ◆, Mn(I); ×, Mn(II); ●, N).

spin-up and spin-down bands. The calculated magnetic moments at each atomic site are in agreement with the observed values, which were reported to be $3.85\mu_B$/atom for Mn(I), $-0.90\mu_B$/atom for Mn(II), $0.0\mu_B$/atom for N at $T = 77$ K, whereas the calculated total moment is about half the observed value ($1.14\mu_B$/unit cell) (Takei *et al* 1962). To obtain the magnetic moment for mixed compounds $Mn_4N_{1-x}C_x$, we adopt the rigid-band model for a replacement of N atoms by C atoms, i.e. we simply shift the Fermi level to lower energies with increasing x. The calculated moments at each atomic site of $Mn_4N_xC_{1-x}$ are shown in figure 7. The results are in agreement with the observed values for $x = 0.25$ (Takei *et al* 1962), but the calculated total moment is about half the observed value.

One of the physical quantities which is directly related to the density of states at the Fermi level, $\rho(E_F)$, is the electronic specific heat coefficient γ defined by $\gamma = \frac{1}{3}\pi^2 k_B^2 \rho(E_F)$. By making use of $\rho(E_F)$ obtained for the ferrimagnetic state of Mn_4N, γ is estimated to be 14.4 mJ K^{-2} mol^{-1}. This value is smaller by a factor of 3

than the experimental value, $\gamma_{exp} = 42 \pm 2\,mJ\ K^{-2}\,mol^{-1}$ (Garcia *et al* 1983). The discrepancy may be remedied by taking into account the effect of the mass enhancement due to the electron–electron interaction.

Acknowledgments

This work is supported by a Grant-in-Aid from the Ministry of Education, Science and Culture of Japan. The authors would like to express their sincere thanks to Professor A Yanase for providing them with the computer program that he developed.

References

Chadi D J and Cohen M L 1973 *Phys. Rev.* B **8** 5747
Fruchart D, Givord D, Convert P, l'Hériter P and Senatue J P 1979 *J. Phys. F: Met. Phys.* **9** 2431
Garcia J, Bartolome J, Gonzales D, Navarro R and Fruchart D 1983 *J. Chem. Thermodyn.* **15** 465
Gunnarsson O and Lundqvist B I 1976 *Phys. Rev.* B **13** 4274
Jepsen O and Andersen O K 1971 *Solid State Commun.* **9** 1763
Lehmann G and Taut M 1972 *Phys. Status. Solidi* b **54** 469
Mekata M 1962 *J. Phys. Soc. Japan* **17** 796
Morgan E R 1954 *J. Met.* **6** 983
Motizuki K and Nagai H 1988 *J. Phys. C: Solid State Phys.* **21** 5259
Suzuki N, Yamasaki T and Motizuki K 1988 *J. Phys. C: Solid State Phys.* **21** 6133
Takei W J, Heikes R R and Shirane G 1962 *Phys. Rev.* **125** 1893